Artigo

Development of Intensity-Duration-Frequency Curves of Intense Rainfall With Emphasis on the Behavior of the Upper Tail of the Distribution

Wagner Alessandro Pansera[1] (iD), Benedito Martins Gomes[2], Eloy Lemos de Mello[2],
João Carlos Cury Saad[3]

[1]*Departamento de Engenharia Civil, Universidade Tecnológica Federal do Paraná, Toledo, PR, Brazil.*

[2]*Centro de Ciência Exatas e Tecnológicas, Universidade Estadual do Oeste do Paraná, Cascavel, PR, Brazil.*

[3]*Departamento de Engenharia Rural e Socioecomia, Faculdade de Ciências Agronômicas, Universidade Estadual Paulista "Júlio de Mesquita Filho", Botucatu, SP, Brazil.*

Abstract

The design and management of various hydraulic structures (such as stormwater drains, bridges and dams) require the estimation of rainfall with duration of a few minutes up to 24 h or more. Intensity-duration-frequency (IDF) curves links probability of occurrence to a given rainfall intensity. The procedure for obtaining IDF curves basically involves two steps: (i) frequency analysis for different durations and (ii) modeling of IDF curves. In the first step, this study aimed to adequately select the upper tail weight of the following distributions: generalized extreme value (GEV), generalized logistic (GLO) and generalized Pareto (GPA). In the second step, this study aimed to evaluate the performance of three models of IDF curves. The traditional model (M1) was compared with empirical model (M2) and a second-order polynomial model (M3). To perform this study, rainfall data from the city of Caraguatatuba (São Paulo state, Brazil) for the period between 1971 and 2001 were used, for time intervals between 10 and 1440 min. The main conclusions were: (i) GLO and GEV had heavy upper tail while GPA had light upper tail, impacting quantiles with $T > 100$ years; (ii) M3 presents errors lower than M1 for return periods greater than 100 years.

Keywords: design rainfall, extreme values, LH moments.

Desenvolvimento de Curvas de Intensidade-Duração-Frequência de Chuvas Intensas com Ênfase no Comportamento da Cauda Superior da Distribuição

Resumo

O projeto e gestão de várias estruturas hidráulicas (tais como: drenos pluviais, pontes e barragens) requerem a estimativa da precipitação com duração de alguns minutos até 24 horas ou mais. As curvas de intensidade-duração-frequência (IDF) vinculam a probabilidade de ocorrência a uma determinada intensidade de chuva. A obtenção das curvas IDF envolve duas etapas: (i) análise da freqüência para diferentes durações e (ii) modelagem das curvas IDF. Na primeira etapa, este estudo teve como objetivo selecionar adequadamente o peso da cauda superior das seguintes distribuições: valor extremo generalizada (GEV), logística generalizada (GLO) e Pareto generalizado (GPA). Na segunda etapa, o objetivo foi avaliar o desempenho de três modelos de curvas IDF. O modelo tradicional (M1) foi comparado com o modelo empírico (M2) e um modelo polinomial de segunda ordem (M3). Para a realização deste estudo, foram utilizados os dados pluviométricos da cidade de Caraguatatuba-SP para o período de 1971 a 2001, para intervalos de tempo entre 10 e 1440 min. As principais conclusões foram: (i) GLO e GEV tiveram caudais pesados enquanto a GPA caudal leve, impactando quantis com $T > 100$ anos; (ii) M3 apresenta erros menores que M1 para períodos de retorno maiores que 100 anos.

Palavras-chave: chuva de projeto, valores extremos, momentos LH.

Autor de correspondência: Wagner Alessandro Pansera, pansera@utfpr.edu.br.

1. Introduction

The design and management of various hydraulic structures, particularly urban drainage systems, require information on the probability of annual maximum rainfall occurring with durations of a few minutes up to 24 h or more (Nguyen *et al.*, 2017). Knowledge of rainfall characteristics allows for safer designs of mechanical structures of soil conservation, such as dams, terraces and drainage projects (Silva *et al.*, 2018). A common way to obtain design rainfall is through intensity-duration-frequency (IDF) curves.

The IDF curves are derived by fitting extreme rainfall quantiles, obtained from frequency analysis methods, by means of parametric equations (You; Tung, 2018). Such equations make it possible to obtain rainfall intensity values (i) as a function of duration (t) and return period (T) (or frequency), and some adjustable parameters (García-Marín *et al.*, 2019). In this sense, IDF curves link probability of occurrence to a given rainfall intensity based on time series with different durations, fitted by a probability distribution function (Faridzad *et al.*, 2018).

The first step for the development of IDF curves is the frequency analysis of the maximum annual rainfall for different durations. The main challenge is to select a suitable distribution that could describe well the rainfall data in each duration. For this purpose, the following distributions can be used: generalized extreme values (GEV), generalized logistics (GLO) and generalized Pareto (GPA) (Hajani and Rahman, 2018; Mamoon and Rahman, 2017; Nguyen *et al.*, 2017).

The upper tail behavior of the GEV, GLO, and GPA distributions may be light, moderate or heavy, depending on the value of the shape parameter (Rao and Hamed, 2000). Papalexiou and Koutsoyiannis (2013) fitted GEV in approximately 15,000 series of annual daily maximum rainfall spread across the globe and pointed out that heavy upper tails should be preferred instead of moderate and light. In Brazil, it is very common to use the Gumbel distribution, one of the possible forms of GEV, with moderate upper tail (Back, 2010; Back *et al.*, 2012; Dorneles *et al.*, 2019; Garcia *et al.*, 2011; Martins *et al.*, 2013; Silva and Araújo, 2013). Quadros *et al.* (2011) performed rainfall frequency analysis for different durations in the city of Cascavel (state of Paraná, Brazil) and observed that Gumbel underestimates GEV for large return periods. This occurred because GEV had a heavier upper tail than Gumbel.

There are few studies using GLO or GPA distributions in the derivation of IDF relations in Brazil (Guimarães and Naghettini, 1998). As GPA has an intermediate upper tail behavior between GEV and GLO (Hosking and Wallis, 1997), it is interesting to evaluate the fitting of the three distributions. Moreover, there have been limited studies on the selection of best fit distribution in design rainfall estimation (Mamoon and Rahman, 2017), mainly based on the upper tail behavior (Nguyen *et al.*, 2017). In this sense, it is very important to select properly the distribution that best describes the rainfall data, because the wrong choice of upper tail behavior can severely underestimate design rainfall, leading to failures and other negative consequences. Overestimation can also be a possibility, with negative consequences in terms of cost.

Once the probability distribution is selected, the quantiles associated with the given return periods are estimated. Afterwards, the model that relates intensity-duration to the respective return periods should be selected. The commonly-used model was proposed by Bernard (1932). However, there are little-explored alternative models, such as the second-order polynomial (Hajani and Rahman, 2018) or the model presented in Pfafstetter (1957). Pansera *et al.* (2020) conducted a study comparing these three models and identified that alternative models can perform better than its traditional counterpart.

Thus, it is possible to summarize the process of obtaining the IDF relations in two steps: (i) frequency analysis for each duration and (ii) estimate the adjustable parameters of IDF model. In the first step, this study aimed to adequately select the upper tail weight for GEV, GLO and GPA distributions using a modified version of the descriptive capacity test presented by Nguyen *et al.* (2017). In the second step, the objective was to evaluate the performance of two alternative IDF models in comparison with the traditional model.

2. Material and Methods

2.1. Rainfall data

We used rainfall data from the municipality of Caraguatatuba (São Paulo state, Brazil) obtained and distributed by Martins *et al.* (2017). The study region can be classified by Köppen system as Af type, i.e., tropical rainforest climate (Santos and Galvani, 2019). The raingauge is located at altitude of 20 m, latitude 23°38' S and longitude 45°26' W. Rainfall data refer to the period from 1971 to 2001 for the following time intervals: 10, 20, 30, 60, 120, 180, 360, 720, 1080 and 1440 min. The stationarity of the rainfall series was verified using Mann-Kendall test, more details in Ibrahim (2019).

2.2. Generalized distributions

The stochastic modeling of the rainfall data was performed using the GEV, GLO and GPA distributions. Such distributions are characterized by three parameters, position, scale and shape, according to the following equations:

$$x_{GEV}(T) = u + \frac{\alpha}{k}\left[1 - \left\{-\ln\left(1 - \frac{1}{T}\right)\right\}^{k}\right] \qquad (1)$$

$$x_{GLO}(T) = u + \frac{\alpha}{k}\left[1 - (T-1)^{-k}\right] \qquad (2)$$

$$x_{GPA}(T) = u + \frac{\alpha}{k}\left[1 - T^{-k}\right] \qquad (3)$$

in which x = quantile of the distribution; T = Return period; u = Position parameter; α = Scale parameter; k = Shape parameter.

The quantiles of the generalized distributions were compared with the quantiles of the Gumbel distribution (Elsebaie, 2012):

$$x_{GUM} = \overline{X} + \left\{0,7797 \times \left[-\ln\left(\ln\left(\frac{T}{T-1}\right)\right)\right] - 0,45\right\} \times S \qquad (4)$$

in which $\overline{X}$ = sample mean and S = sample standart deviation.

2.2.1. Parameter estimation

To calculate the quantiles, it is necessary to estimate the distributions' parameters. For this purpose, LH moments were used, a generalization of the L moments (Wang, 1997). The LH moments provide more weightage to the larger values in the rainfall series and hence are expected to provide better fits to the upper tail of the distribution (Haddad; Rahman, 2008).

To calculate the sample LH moments, with an ordered random sample of size n, represented by $x_{1:n} \leq x_{2:n} \leq \ldots \leq x_{n:n}$, the expressions are used (Wang, 1997):

$$\hat{\lambda}_1^\eta = \frac{1}{{}^n C_{\eta+1}} \sum_{i=1}^{n} {}^{i-1}C_\eta x_{(i)} \qquad (5)$$

$$\hat{\lambda}_2^\eta = \frac{1}{2}\frac{1}{{}^n C_{\eta+2}} \sum_{i=1}^{n} \left({}^{i-1}C_{\eta+1} - {}^{i-1}C_\eta {}^{n-1}C_1\right) x_{(i)} \qquad (6)$$

$$\hat{\lambda}_3^\eta = \frac{1}{3}\frac{1}{{}^n C_{\eta+3}} \sum_{i=1}^{n} \Big({}^{i-1}C_{\eta+2} - 2{}^{i-1}C_{\eta+1}{}^{n-1}C_1 \\ + {}^{i-1}C_\eta {}^{n-i}C_2\Big) x_{(i)} \qquad (7)$$

In which: $\hat{\lambda}_1^\eta, \hat{\lambda}_2^\eta, \hat{\lambda}_3^\eta$ = sample LH moments; η = level of LH moments (0, 1, 2, 3 or 4); ${}^m C_j = \binom{m}{j}$ and ${}^m C_j = 0$ when $j > m$.

By normalizing the LH moments, the coefficient of skewness is obtained:

$$\hat{\tau}_3^\eta = \frac{\hat{\lambda}_3^\eta}{\hat{\lambda}_2^\eta} \qquad (8)$$

The populational LH moments of the GEV are (Wang, 1997):

$$\lambda_1^\eta = u + \frac{\alpha}{k}\left[1 - \Gamma(1+k)(\eta+1)^{-k}\right] \qquad (9)$$

$$\lambda_2^\eta = \frac{(\eta+2)\alpha\Gamma(1+k)}{2!k}\left[-(\eta+2)^{-k} + (\eta+1)^{-k}\right] \qquad (10)$$

$$\tau_3^\eta = \frac{(\eta+3)}{3(\eta+2)}\frac{\left[-(\eta+4)(\eta+3)^{-k} + 2(\eta+3)(\eta+2)^{-k} - (\eta+2)(\eta+1)^{-k}\right]}{\left[-(\eta+2)^{-k} + (\eta+1)^{-k}\right]} \qquad (11)$$

In which Γ = represents the full gamma function.

The populational LH-moments of the GLO are (Meshgi and Khalili, 2009):

$$\lambda_1^\eta = u + \frac{\alpha}{k}\left[1 - \frac{\Gamma(1+k)\Gamma(\eta+1-k)}{\eta!}\right] \qquad (12)$$

$$\lambda_2^\eta = \frac{(\eta+2)\alpha\Gamma(1+k)}{2!k}\left[\frac{\Gamma(\eta+2-k)}{(\eta+1)!} + \frac{\Gamma(\eta+1-k)}{\eta!}\right] \qquad (13)$$

$$\tau_3^\eta = \frac{(\eta+3)}{3(\eta+2)}\frac{\left[-\frac{(\eta+4)\Gamma(\eta+3-k)}{(\eta+2)!} + 2\frac{(\eta+3)\Gamma(\eta+2-k)}{(\eta+1)!} - \frac{(\eta+2)\Gamma(\eta+1-k)}{\eta!}\right]}{\left[\frac{\Gamma(\eta+2-k)}{(\eta+1)!} + \frac{\Gamma(\eta+1-k)}{\eta!}\right]} \qquad (14)$$

The populational LH moments of the GLO are (Meshgi and Khalili, 2009):

$$\lambda_1^\eta = u + \frac{\alpha}{k}\left[1 - \frac{\Gamma(1+k)\Gamma(\eta+1-k)}{\eta!}\right] \quad (15)$$

$$\lambda_2^\eta = \frac{(\eta+2)\alpha\Gamma(1+k)}{2!k}\left[\frac{\Gamma(\eta+2-k)}{(\eta+1)!} + \frac{\Gamma(\eta+1-k)}{\eta!}\right] \quad (16)$$

$$\tau_3^\eta = \frac{(\eta+3)}{3(\eta+2)}\frac{\left[-\frac{(\eta+4)\Gamma(\eta+3-k)}{(\eta+2)!} + 2\frac{(\eta+3)\Gamma(\eta+2-k)}{(\eta+1)!} - \frac{(\eta+2)\Gamma(\eta+1-k)}{\eta!}\right]}{\left[\frac{\Gamma(\eta+2-k)}{(\eta+1)!} + \frac{\Gamma(\eta+1-k)}{\eta!}\right]} \quad (17)$$

The parameters of the GEV, GLO and GPA distributions are obtained in three steps. Step one, we calculate k by resolving the equality $\tau_3^\eta = \hat{\tau}_3^\eta$. Step two, equalizing $\lambda_2^\eta = \hat{\lambda}_2^\eta$ we can calculate α. Step three, equalizing $\lambda_1^\eta = \hat{\lambda}_1^\eta$ u is calculated.

2.3. Choosing optimal upper tail weight

Wang (1997) recommends that the values of $\eta = 0$, 1, 2, 3 or 4 should be tested, i.e., for each distribution there are five sets of parameters. The choice of the value η has an impact on the shape parameter, affecting the weight of the upper tail and, consequently, the value of the estimated quantiles. To choose the most appropriate value of η, a modified version of the descriptive capacity test (MDCT) proposed by Nguyen *et al.* (2017) was used. The MDCT is based on the following indicators: modified prediction absolute error (MPAE), root mean square error (RMSE), relative root mean square error (RRSE), maximum absolute error (MAE) and correlation coefficient (CC):

$$MPAE = \frac{2}{n}\sum\nolimits_{i={}^n/_2}^{n}\left|x_{(i)} - \hat{x}_{(i)}\right| \quad (18)$$

$$RMSE = \left[\frac{2}{n}\sum\nolimits_{i={}^n/_2}^{n}\left(x_{(i)} - \hat{x}_{(i)}\right)^2\right]^{0,5} \quad (19)$$

$$RRMSE = \left[\frac{2}{n}\sum\nolimits_{i={}^n/_2}^{n}\left(\frac{x_{(i)} - \hat{x}_{(i)}}{\hat{x}_{(i)}}\right)^2\right]^{0,5} \quad (20)$$

$$MAE = max\left(\left|x_{(i)} - \hat{x}_{(i)}\right|\right) \ (from \ n/2 \ to \ n) \quad (21)$$

$$CC = \frac{cov\left(x_{(i)}, \hat{x}_{(i)}\right)}{S\left(x_{(i)}\right) \times S\left(\hat{x}_{(i)}\right)} \ (from \ n/2 \ to \ n) \quad (22)$$

in which n is the number of observations, $x_{(i)}$ are the observations in ascending order, $\hat{x}_{(i)}$ are the quantiles esti-

mated by the distributions using the plot position $p = i/(n+1)$, cov is the covariance and S is the standard deviation. The reason for using $n/2$ is to investigate the effect of η (0 to 4) beyond the 50-th percentile.

After calculating the five indicators, a ranking system was used. The ranking score was assigned to each η according to the calculated value for each indicator. To the η with the lowest RMSE, RRSE, MAE, MAPE or higher CC, rank 1 is assigned. In addition, the overall rank associated with each η was calculated by adding to the individual rank.

2.4. Modeling of intensity-duration-frequency relations

After choosing the probability distribution for each duration, the quantiles were estimated. With the values obtained from intense rainfall for different durations and return periods, points were generated to estimate the IDF curves. Three models were used: traditional (M1), empirical (M2) and second-order polynomial (M3).

$$i = \frac{P1 \times T^{P2}}{(t + P3)^{P4}} \ (M1) \quad (23)$$

$$i = \frac{1}{t}\left(T^{P1 + \frac{P2}{T^{P3}}}\right)\left[P4 \times t + P5 \times \log_{10}^{(1+P6 \times t)}\right] \ (M2) \quad (24)$$

$$\ln(i) = P1 \times \ln(t)^2 + P2 \times \ln(t) + P3 \ (M3) \quad (25)$$

in which i - rainfall intensity (mm h^{-1}); T - return period (years); t - rainfall duration (min); P - Fitting parameters of the model. The parameters of each model were estimated using the ordinary least squares method.

3. Results and Discussion

Through Mann-Kendall test at significance level of 5%, it can be considered that the rainfall series are stationary. In the sequence, the parameters of the GEV, GLO and GPA distributions were estimated using LH moments

(for η = 0, 1, 2, 3 and 4). As an example, Fig. 1 shows the quantiles obtained by the GEV for a duration of 10 min.

It can be seen in Fig. 1 that for $T \leq 100$ years, the behavior of the GEV is similar in all η values. However, for $T > 100$ years, the GEV upper tail are more influenced by the value of η. Simple visual inspection does not allow to properly choose the value of η to estimate quantiles with $T > 100$ years. This is because there is not enough information to make this choice. This demonstrates the importance of a more objective assessment using numerical comparison criteria (Nguyen *et al.*, 2017).

The modified descriptive capacity test (MDCT) was applied to select the most appropriate level of the LH moments for the 10 min rainfall using GEV distribution, as presented in Table 1. In this example, we selected η = 4, as it presented the lowest overall rank. This procedure was repeated for the other durations and was also performed for GLO and GPA distributions. Next, Fig. 2 was created to compare and evaluate the behavior of the upper tail through the application of MDCT.

It Fig. 2 is possible to observe that the shape parameter of the GEV was essentially negative, presenting positive value only in the durations 30 and 60 min. According to Stedinger *et al.* (1993), when the shape parameter is within the range of −0.03 to 0.03 the shape of the GEV resembles that of Gumbel. All values of the shape
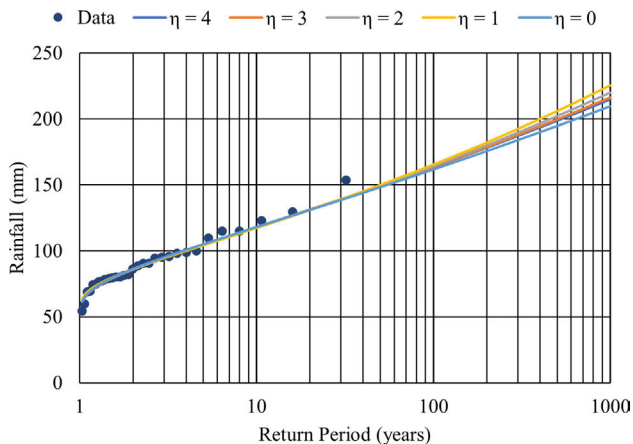
parameter were outside this range and most durations presented heavy upper tail ($k < -0.03$). The GLO distribution presented negative shape parameter (except for the duration of 60 min), therefore, it also presented heavy upper tail.

The GPA distribution showed a 50% positive and 50% negative shape parameter (Fig. 2), i.e., it was divided between light and heavy upper tail. In this sense, unlike GEV and GLO, GPA is not a good choice for the studied rainfall data, as it has a strong tendency to present light tails and in the study of maximum annual rainfall, heavy upper tail should be chosen (Papalexiou and Koutsoyiannis, 2013). This may have occurred because GPA performs better in peaks-over-threshold series than in annual maximum series (Ibrahim, 2019).
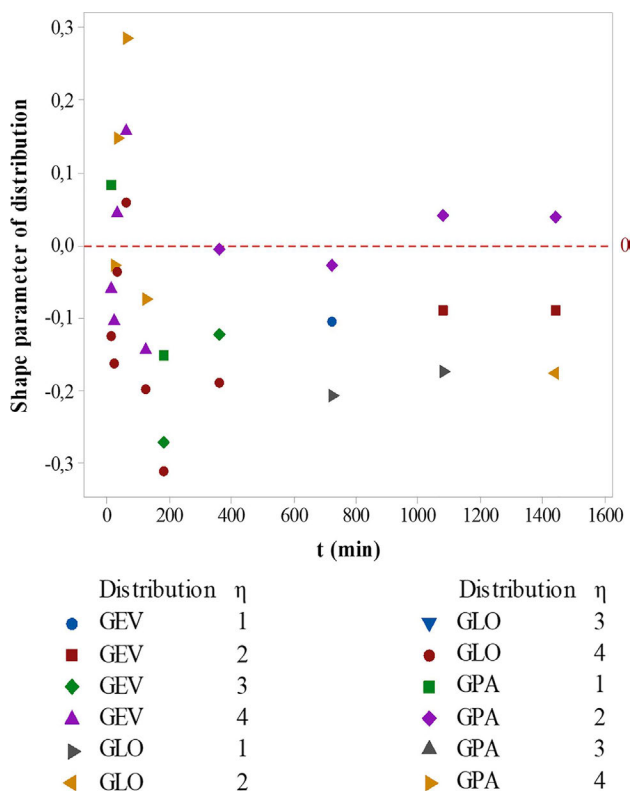

Figure 1 - Quantiles generated by the GEV for a duration of 10 min.

Figure 2 - Shape parameter and level of LH moments for GEV, GLO and GPA distributions as a function of rainfall duration.

Table 1 - Example of application of modified descriptive capacity test (MDCT) for duration of 10 min using GEV distribution.

	Indicator					Ranking					
η	RMSE	RRSE	MAE	CC	MAPE	RMSE	RRSE	MAE	CC	MAPE	General
0	4.1948	3.2872	13.9881	0.9890	2.6175	5	4	5	5	1	20
1	4.1806	3.3496	13.0629	0.9912	2.7471	4	5	1	1	5	16
2	4.1258	3.2872	13.1544	0.9905	2.6748	3	3	4	2	4	16
3	4.0759	3.2432	13.1359	0.9899	2.6394	2	2	3	3	3	13
4	4.0567	3.2306	13.1034	0.9897	2.6381	1	1	2	4	2	10

It is worth mentioning that η = 0 was not selected in any duration or distribution (Fig. 2), that is, the LH moments were more adequate in modeling intense rainfall than the L moments. This result similar to that of Quadros *et al.* (2011) that pointed out that the L moments were not enough to obtain the best fit in the different durations.

The Fig. 3 shows a comparison of the rainfall intensity estimated by the Gumbel, GEV, GLO and GPA distributions in the return periods of 10, 100, 500 and 1000 years. We can observe that for *T* = 10 years, the four distributions present similar results for all durations studied. For *T* = 100 years, the Gumbel distribution begins to diverge from other distributions, especially in durations of less than 200 min. In the return periods of 500 and 1000 years, the difference between Gumbel and

the GEV, GLO and GPA distributions is evident in almost all durations. This fact corroborates Quadros *et al.* (2011) who also found underestimates in rainfall intensity using Gumbel, when compared to GEV, for high return periods.

The performance of the Gumbel distribution in the upper tail (*T* > 100 years) can be explained due to the absence of the shape parameter, which makes Gumbel less flexible when compared to GEV, GLO or GPA. Therefore, care must be taken in choosing the probability distribution that will be used to estimate rainfall for hydraulic works. Svensson and Jones (2010) point out that return periods greater than 100 years are relevant in the design and in the safety of reservoirs. Euclydes (2011) recommends a 500-year return period in the sizing of small earth dams. As such, the Gumbel distribu-
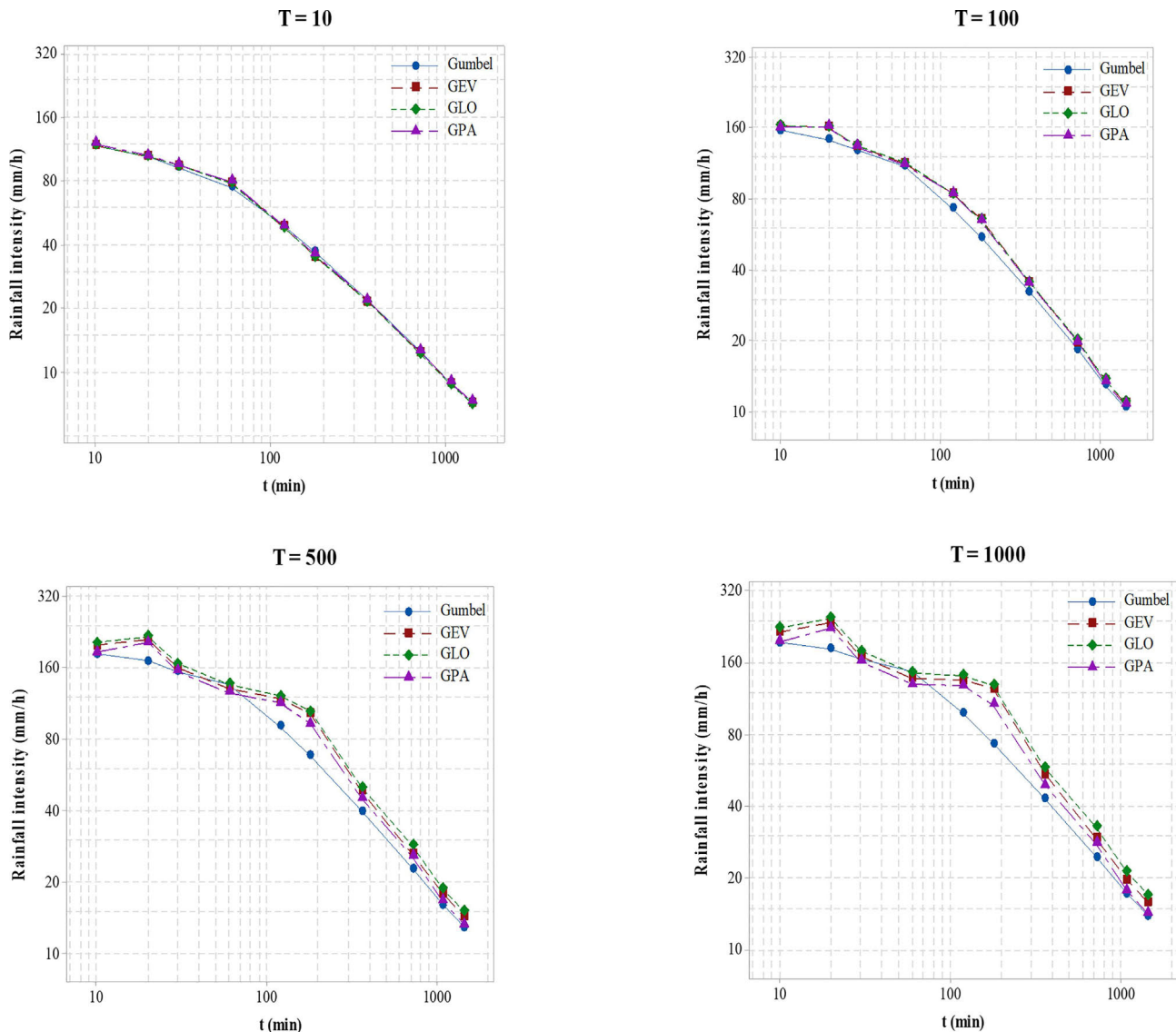

Figure 3 - Comparison of rainfall intensity estimated by Gumbel, GEV, GLO and GPA distributions in the return periods of 10, 100, 500 and 1000 years.

tion is not recommended in these projects. Tucci (2016) indicates the 10-year return period for urban micro drainage projects. The NBR 10844 bill (ABNT, 1989) recommends return periods of 1, 5 and 25 years in the design of rainwater construction facilities. Therefore, when the return period is considered low, the Gumbel distribution can be used without damaging the estimate, given its ease in estimating the intensity of rainfall in various hydraulics works sizing.

Based on the results found, to estimate the parameters of the models of the IDF relations, the return periods were divided into two groups: (i) $T \leq 100$ years and (ii) $T > 100$ years. For group (i) the selected return periods were: 2, 5, 10, 20, 50 and 100 years. For the group (ii) the selected return periods were: 200, 500, 750 and 1000. Thus, the parameters of models M1, M2 and M3 were estimated, according to Table 2.

In addition, the Fig. 4 was created with the objective of evaluating the error made by the models in the different durations in the return periods of 10, 100 and 1000 years. It is observed that the models, in general, presented errors of up to 25%, approximately. For durations of less than 200 min the models had similar behavior. Whenever $T = 10$ years, it is observed that the models may present errors of up to 10%, except M2, which in the duration of 1440 min, generated an error of approximately 25%. M1 and M2 presented similar behavior, in which the greatest errors were observed for $T = 100$ years, in durations greater than 200 min. M3 presented the lowest errors, when compared to M1 and M2, for durations greater than 200 min and $T = 100$ years. For the return period of 1000 years and durations of less than 200 min, the models presented similar behavior, and errors of approximately 20% could have occurred. For durations greater than 200 min, M1 and M3 maintained errors below 10%, since M2 presented errors of the order 20%. Therefore, the conclusion is similar with Hajani and Rahman (2018), that is, the
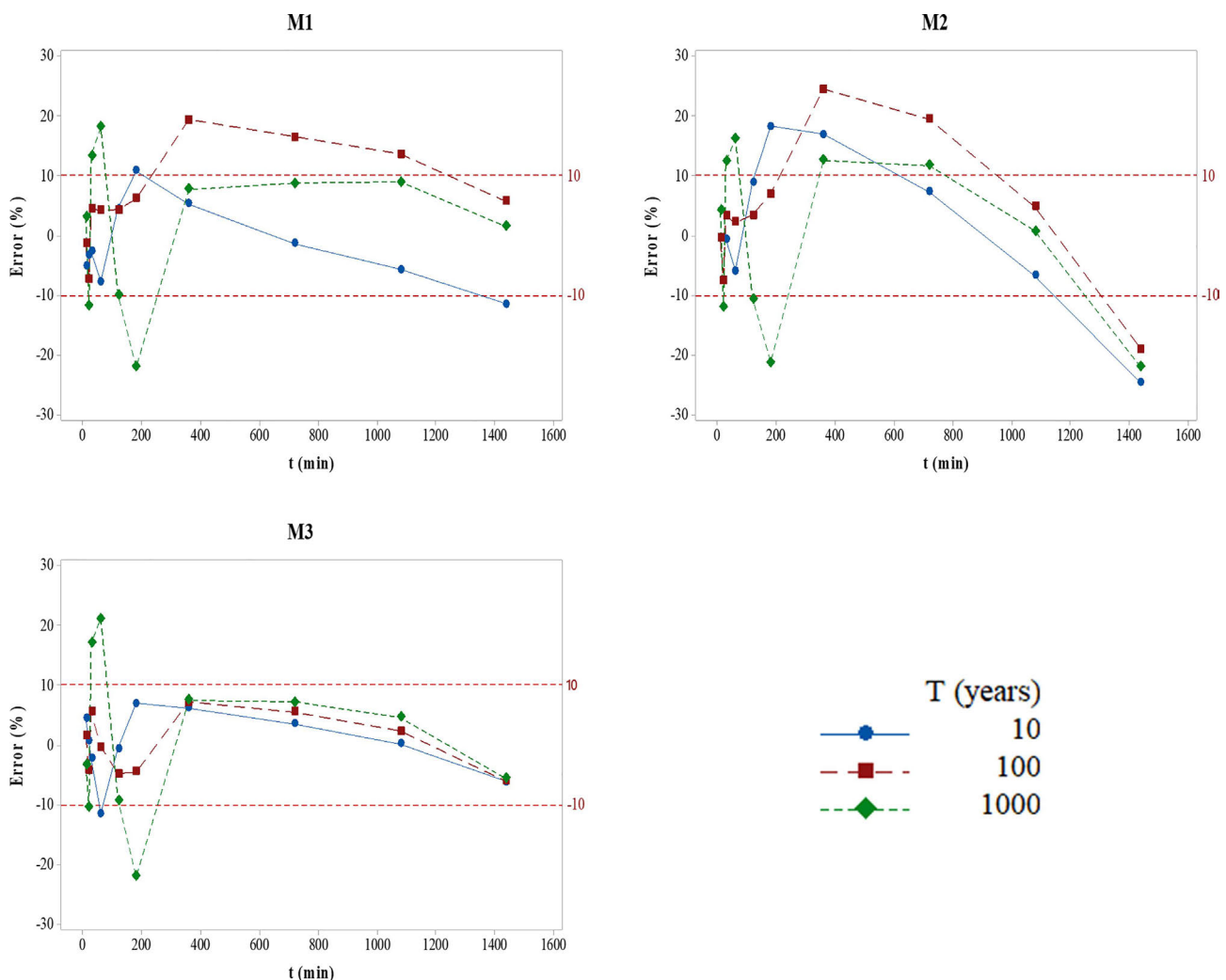

Figure 4 - Error as a function of the duration of the rain for M1, M2 and M2 in the return periods of 10, 100 and 1000 years.

Tabela 2 - Parameter estimation of models M1, M2 and M3.

Model	T (Years)	P1	P2	P3	P4	P5	P6
M1	≤100	8476.661	0.196	86.661	1.045		
	>100	27951.750	0.138	148.572	1.143		
M2	≤100	0.197	0.322	0.401	−3.281	5043.689	0.031
	>100	0.190	0.429	0.285	−3.854	6073.757	0.018
M3	2	−0.052	−0.107	5.001			
	5	−0.074	0.116	4.822			
	10	−0.084	0.221	4.754			
	20	−0.093	0.307	4.701			
	50	−0.102	0.406	4.638			
	100	−0.108	0.476	4.591			
	200	−0.114	0.542	4.543			
	500	−0.122	0.628	4.475			
	750	−0.125	0.666	4.444			
	1000	−0.128	0.692	4.421			

second-order polynomial model presents better results than empirical models, especially for high periods of return.

The performance of the models can be explained by the complexity of the relationship between intensity (i), duration (t) and the return period (T). In models M1 and M2 there is interaction between t and T, in addition, the relationship of i with t and T is nonlinear. On the other hand, the M3 model has a quadratic relationship of i only with t and there is no interaction between t and T. That is, for $T > 100$ years, the simplest form of M3 may have helped to reduce the errors generated by the model, while for the M2 and M1 models it may have helped to increase the error. Further, the number of model parameters may also have contributed as another source of errors.

3. Conclusions

After the analyses carried out in this work, the following conclusions can be reached:

1 - The modified version of the descriptive capacity test was capable to correct select the upper tail weight of the GEV, GLO and GPA distributions.

2 - The GLO and GEV distributions presented heavy upper tail, while the GPA distribution presented light upper tail. This was reflected in quantiles with a return period greater than 100 years. Therefore, design rainfall with a return period greater than 100 years should be estimated using the GEV or GLO distribution.

3 - For return periods of less than 100 years the traditional model (M1) presents good results; for return periods greater than or equal to 100 years, it is recommended to use the second-order polynomial model (M2).

References

ASSOCIAÇÃO BRASILEIRA DE NORMAS TÉCNICAS (ABNT). **NBR 10844: Instalações Prediais de Águas Pluviais**. Rio de Janeiro: ABNT, 13 p., 1989.

BACK, Á.J. Relações intensidade-duração-freqüência de chuvas intensas de Urussanga, SC. **Irriga**, v. 15, n. 2, p. 119-130, 2010. doi

BACK, Á.J.; OLIVEIRA, J.L.R.; HENN, A. Duration-frequency relationships of heavy rainfall in Santa Catarina, Brazil. **Revista Brasileira de Ciência do Solo**, v. 36, n. 3, p. 1015-1022, 2012. doi

BERNARD M. Formulas for rainfall intensities of long duration. **Transactions of the American Society of Civil Engineers**, v. 96, n. 1, p. 592-606, 1932. doi

DORNELES, V.R.; DAMÉ, R.C.F.; TEIXEIRA-GANDRA, C.F.A.; VEBER, P.M.; KLUMB, G.B. *et al.* Modeling of probability in obtaining intensity-duration-frequency relationships of rainfall occurrence for Pelotas, RS, Brazil. **Revista Brasileira de Engenharia Agricola e Ambiental**, v. 23, n. 7, p. 499-505, 2019. doi

ELSEBAIE, I.H. Developing rainfall intensity-duration-frequency relationship for two regions in Saudi Arabia. **Journal of King Saud University - Engineering Sciences**, v. 24, n. 2, p. 131-140, 2012. doi

EUCLYDES, H.P. (coord.). **Atlas Digital das Águas de Minas**. Viçosa: UFV, 2011. Disponível em http://www.atlasdasaguas.ufv.br/home.html, acesso em 10 out. 2021.

FARIDZAD, M.Y.T.; HSU, K.; SOROOSHIAN, S.; XIAO, C. Rainfall frequency analysis for ungauged regions using remotely sensed precipitation information. **Journal of Hydrology**, v. 563, p. 123-142, 2018. doi

GARCIA, S.S.; AMORIM, R.S.S.; COUTO; E.G.; STOPA, W.H. Determinação da equação intensidade-duração-frequência para três estações meteorológicas do Estado de Mato Grosso. **Revista Brasileira de Engenharia Agrícola e Ambiental**, v. 15, n. 6, p. 575-581, 2011. doi

GARCÍA-MARÍN, A.P.; MORBIDELLI, R.; SALTALIPPI, C.; CIFRODELLI, M.; ESTÉVEZ, J. *et al.* On the choice of the optimal frequency analysis of annual extreme rainfall by multifractal approach. **Journal of Hydrology**, v. 575, p. 1267-1279, 2019. doi

GUIMARÃES, M.; NAGHETTINI, M. Análise regional de freqüência e distribuição temporal das tempestades na Região Metropolitana de Belo Horizonte - RMBH. **Revista Brasileira de Recursos Hídricos**, v. 3, n. 4, p. 73-88, 1998.

HADDAD, K.; RAHMAN, A. Investigation on at-site flood frequency analysis in South-East Australia. **The Institution of Engineers**, v. 69, n. 3, p. 59-64, 2008.

HAJANI, E.; RAHMAN, A. Design rainfall estimation: comparison between GEV and LP3 distributions and at-site and regional estimates. **Natural Hazards**, v. 93, n. 1, p. 67-88, 2018. doi

HOSKING, J.R.M.; WALLIS, J.R. **Regional frequency analysis: an approach based on L-moments**. Cambridge University Press, Cambridge, 224 p., 1997.

IBRAHIM, M.N. Generalized distributions for modeling precipitation extremes based on the L moment approach for the Amman Zara Basin, Jordan. **Theoretical and Applied Climatology**, v. 138, n. 1-2, p. 1075-1093, 2019. doi

MAMOON, A.A.L.; RAHMAN, A. Selection of the best fit probability distribution in rainfall frequency analysis for Qatar. **Natural Hazards**, v. 86, n. 1, p. 281-296, 2017. doi.

MARTINS, D.K.N.S.; MAGNI, N.L.G.; QUEIROZ, P.I.B. Comparação de duas metodologias de obtenção da equação de chuvas intensas para a cidade de Caraguatatuba (SP). **Revista DAE**, v. 65, n. 207, p. 34-49, 2017. doi

MESHGI, A.; KHALILI, D. Comprehensive evaluation of regional flood frequency analysis by L- and LH-moments. II. Development of LH-moments parameters for the generalized Pareto and generalized logistic distributions. **Stochastic Environmental Research and Risk Assessment**, v. 23, n. 1, p. 137-152, 2009. doi

NGUYEN, T.H.; OUTAYEK, S.E.; LIM, S.H.; NGUYEN, V.T.V. A systematic approach to selecting the best probability models for annual maximum rainfalls - A case study using data in Ontario (Canada). **Journal of Hydrology**, v. 553, p. 49-58, 2017. doi

PANSERA, W.A.; GOMES, B.M.; SAAD, J.C.C. Desempenho de modelos paramétricos intensidade-duração-frequência

no estudo de chuvas intensas. **Irriga**, v. 25, n. 1, p. 102-111, 2020. doi

PAPALEXIOU, S.M.; KOUTSOYIANNIS, D. Battle of extreme value distributions: A global survey on extreme daily rainfall. **Water Resources Research**, v. 49, n. 1, p. 187-201, 2013. doi

PFAFSTETTER, O. **Chuvas Intensas no Brasil**. Brasília: Departamento Nacional de Obras e Saneamento, 246 p., 1957.

QUADROS, L.E.; QUEIROZ, M.M.F.; VILAS BOAS, M.A. Distribuição de frequência e temporal de chuvas intensas. **Acta Scientiarum - Agronomy**, v. 33, n. 3, p. 401-410, 2011. doi

RAO, A.R.; HAMED, K.H. **Flood Frequency Analysis**. CRC Press: Boca Raton, 2000.

SANTOS, D.D.; GALVANI, E. Proposta para determinação de eventos extremos de chuva no litoral norte paulista. **Revista Brasileira de Climatologia**, v. 25, p. 702-718, 2019. doi

SILVA, S.R.; ARAÚJO, G.R.S. Algoritmo para determinação da equação de chuvas intensas. **Revista Brasileira de Geografia Física**, v. 6, n. 5, p. 1371-1383, 2013.

SILVA, J.B.L.; CÂNDIDO, F.A.; PIRES, L.C.; FRANÇA, L.C.J. Nota técnica: Equações de intensidade, duração e frequência de chuvas máximas para o Estado do Rio Grande do Norte, Brasil. **Revista Engenharia na Agricultura - Reveng**, v. 26, n. 2, p. 160-170, 2018. doi

STEDINGER, J.R.; VOGEL, R.M.; FOUFOULA-GEORGIOU, E. Frequency analysis of extreme events. In: MAIDMENT, D.R. **Handbook of Hydrology**. New York: McGraw-Hill, p. 18.1-18.66, 1992.

SVENSSON, C.; JONES, D.A. Review of rainfall frequency estimation methods. **Journal of Flood Risk Management**, v. 3, n. 4, p. 296-313, 2010. doi

TUCCI, C. Regulamentação da drenagem urbana no Brasil. **Revista de Gestão de Água da América Latina**, v. 13, n. 1, p. 29-42, 2016.

WANG, Q.J. LH moments for statistical analysis of extreme events. **Water Resources Research**, v. 33, n. 12, p. 2841-2848, 1997. doi

YOU, L.; TUNG, Y.K. Derivation of rainfall IDF relations by third-order polynomial normal transform. **Stochastic Environmental Research and Risk Assessment**, v. 32, n. 8, p. 2309-2324, 2018. doi